

# Investigation of phase behaviour in the melt in blends of single-site based linear polyethylene and ethylene–1-alkene copolymers

B.S. Tanem<sup>a,\*</sup>, A. Stori<sup>b,1</sup>

<sup>a</sup>Norwegian University of Science and Technology, Department of Machine Design and Materials Technology, Trondheim, Norway

<sup>b</sup>Sintef Materials Technology, Department of Polymer and Composites, Oslo, Norway

Received 31 July 2000; received in revised form 5 October 2000; accepted 31 October 2000

## Abstract

In this work, results obtained by blending different single-site based linear polyethylenes with different ethylene–1-alkene copolymers are presented. Several morphology maps are created, and phase separation in the blends is detected. The extent of phase separation is found to be significantly wider in both temperature and composition than reported earlier, and no closed loops of phase separation is observed. This might partly be explained from the more even comonomer distribution found in single-site materials compared to materials made by other processes. The type of short chain branches is found to be of limited (if any) importance to the extent of phase separation while a difference in molecular weight of the blend components seems to affect the extent of phase separation. Furthermore, in blends containing butyl branches, the extent of phase separation is found to be reduced if the amount of comonomer is reduced. © 2001 Elsevier Science Ltd. All rights reserved.

*Keywords:* Polyethylene blends; Single-site catalysts; Phase separation

## 1. Introduction

The phase behaviour in the melt of polyethylene blends has attracted considerable interest in recent years. The most studied systems involve blends of linear polyethylene (LPE) and lightly branched polyethylene. An experimental technique has been developed [1–22] which is believed to be able to discriminate between a separated melt and a homogeneous melt. This technique involves examination of rapidly quenched melts in the solid state using differential scanning calorimetry (DSC) and transmission electron microscope (TEM). By using this method, evidence of phase separation of a characteristic type is observed in the melt for a large number of blends of linear and branched polyethylene, where the amount of branching is between 1 and 9 mol%. The phase separation is found to occur on a large spatial scale. The minority domains are observed to be a few microns in diameter and separated on the same scale [18]. The dimension of the separated phases are probably too large to be visible in small-angle neutron scattering (SANS) experiments [23]. Phase separation has, however,

been observed by SANS in blends of linear and branched polyethylene [24–30], but only in blends containing more than 12 mol% comonomer in the branched blend component. In such blends the phase separation is observed to be somewhat different and occurs on a different scale [7].

Others [24] have argued against this method, claiming that the observed segregation is a crystallisation-induced segregation from a homogeneous melt. It has, however, been established that the diffusion rates of the blend components are too slow to account for the phase separation observed in DSC and TEM [6,10]. While the quenching takes less than a second, it will take several minutes to generate the phases observed in TEM. Due to the extremely fast quenching a crystallisation induced separation of the blend component is not believed to occur. Furthermore, it has been observed that the separated phases ripen with storage time in the melt [14]. Most of the earlier published work has made use of less well-defined material, i.e. LPE with large polydispersities, LLDPE with heterogeneous distribution of comonomer or LDPE with more than one branch type. The introduction of single-site materials have made it possible to synthesise materials with a more even distribution of chain branching along the chains and a more narrow distribution of molecular weights, as compared to materials produced by other processes, e.g. Ziegler–Natta based catalytic processes. It has been observed that

\* Corresponding author. Fax: +47-73-59-41-29.

E-mail addresses: bjorn.s.tanem@immtek.ntnu.no (B.S. Tanem), aage.stori@matek.sintef.no (A. Stori).

<sup>1</sup> Fax: +47-22-06-7350.

Table 1  
Characterisation of the single-site materials used in this work

	$M_w^a$ g/mol	$M_w/M_n^b$	SCB <sup>c</sup> (mol%)
LPE(26k)	26 000	5	–
LPE(435k)	435 000	3.2	–
EB(5.3)	95 000	2.3	5.3
EB1(7.7)	60 000	4.5	7.7
EB2(7.7)	95 000	2.4	7.7
EH	95 000	3.0	
EH(4.9)	110 000	3.6	4.9
EH(4.0)	105 000	3.1	4.0
EH(3.9)	370 000	2.5	3.9
EO(4.8)	100 000	2.4	4.8

<sup>a</sup> Weight-average molecular weight determined from GPC.

<sup>b</sup> Polydispersity determined from GPC.

<sup>c</sup> Amount of short chain branches (in mol%) determined from FTIR and NMR.

co-crystallisation in blends of LPE and single-site based ethylene–butene copolymer occurs in a narrower blend compositions than in blends of LPE and Ziegler–Natta based ethylene–butene copolymer [31–34]. It is therefore reasonable to expect that the phase behaviour in the melt is different in blends including single-site materials compared to blends of materials made by other processes. Others have, however, concluded that blends of single-site materials behave similar in the melt compared to blends of materials made by other processes [18].

In this work, results obtained by blending different single-site based LPEs with different single-site based ethylene–1-alkene copolymers are presented. The phase separation that is observed is found to be wider in both temperature and composition compared to earlier presented results.

## 2. Experimental

### 2.1. The materials

Two different LPEs are employed in this work. These samples will be denoted by the weight-average molecular weight, i.e. LPE(26k) and LPE(435k), where 26k indicates that the molecular weight of the sample LPE(26k) is 26 000 g/mol. LPE(26k) is supplied from Borealis AS, while LPE(435k) is made at NTNU in Norway. Furthermore, three different ethylene–butene copolymers are used. These copolymers are denoted EB(5.3), EB1(7.7) and EB2(7.7). The letters indicate that butene is used as comonomer, while the number in the parentheses gives the amount of comonomer (in mol%) in the copolymers. EB(5.3) and EB2(7.7) are commercial EXACT copolymers supplied from EXXON Chemicals, while EB1(7.7) is an extracted fraction of a copolymer supplied from Borealis AS.

In addition, four different ethylene–hexene copolymers are used in this work. These are denoted EH, EH(3.9),

EH(4.0) and EH(4.9), where the letters and number in the parentheses are given for the same reason as for the ethylene–butene copolymers (the comonomer content in EH was not determined). EH is an extracted fraction of a copolymer supplied by Borealis AS, EH(3.9) is a copolymer supplied from Borealis AS, EH(4.9) is a commercial EXACT copolymer supplied from EXXON Chemicals, while EH(4.0) is a copolymer made at NTNU in Norway. Finally, an ethylene–octene copolymer, denoted EO(4.8) is used, which is an extracted fraction from a commercial EXACT copolymer supplied from EXXON Chemicals. The samples together with relevant information are listed in Table 1.

### 2.2. Size exclusion chromatography (GPC)

Weight-average molecular weight,  $M_w$ , as well as polydispersity ( $M_w/M_n$ ) were determined on a Waters 150 CVplus no.1115 GPC, equipped with three HT6E styragel columns from Waters, a RI detector and Viscotek viscometer. The polymer was dissolved in TCB (1,2,4-trichlorobenzene) stabilised with BHT (2,6-di-*tert*-butyl-*p*-cresol) and heated for 4 h at 140°C in an oven before put into the GPC. The samples were held at 140°C in the GPC for 3 h before the first injection. The column temperature was 140°C. The flow rate was 1.0 ml/min. The instrument was calibrated against narrow standard polystyrene samples. Molecular weights were obtained by universal calibration.

### 2.3. Comonomer content

The comonomer content of three of the samples used in this study was determined from <sup>13</sup>C NMR. The samples were weighted into 5 mm outer diameter NMR tubes, dissolved in deuterated *ortho*-dichlorobenzene, saturated with N<sub>2</sub> and the tubes sealed. The samples were then heated in an oven to 175°C to make the solution homogeneous before the samples were transferred to the NMR instrument. In the NMR instrument the samples were kept at 150°C for 30 min before cooling to 130°C, and the FID obtained. A delay of 30 s and an acquisition time of 2 s was employed to ensure quantitative data acquisition. Five hundred and twelve scans were employed on each sample. 1H decoupling using WALTZ decoupling pulse sequence was used under the delay as well as the acquisition to remove coupling between protons and carbon nuclei and to give maximum NOE enhancement. The obtained FIDs were Fourier transformed and integrated. The amount of branches in mol% was calculated according to Hansen et al. [35].

The comonomer content of the remaining samples was determined from FTIR by Borealis AS. Films with thickness of about 230 μm were pressed from the samples using a Graseby Specac IR film press at 150°C. The films prepared were analysed immediately after pressing. Two IR spectra were acquired from each sample using a Nicolet Magna 550

FTIR spectrometer purged with dry nitrogen and equipped with a DTGS detector. Resolution was  $2\text{ cm}^{-1}$ , and the number of scans was 128. Data collection and handling was carried out with Nicolet Omnic software using a macro written with Visual Basic. The comonomer content was determined using the total methyl absorption at around  $1378\text{ cm}^{-1}$ . The measured absorbance was divided by film thickness and the comonomer content was obtained from a calibration curve constructed with a series of unimodal Z–N and metallocene PE samples analysed by  $^{13}\text{C}$  NMR.

#### 2.4. Extraction

Ten grams of the sample (in powder) was introduced in a glass reactor kept at  $70^\circ\text{C}$  using circulating silicon oil and 400 ml of boiling solvent (see below) was added. The slurry was subjected to intensive stirring by a vibromixer for 30 min. before the solvent along with the extracted polymer was allowed to flow out from the reactor. Another 500 ml of boiling solvent was added and the extraction step repeated. The solution was thereafter allowed to evaporate for a few hours before it was reheated, followed by precipitation of the extracted polymer in an excess amount of cold methanol, a non-solvent. EO(4.8) and EB1(7.7) are extracted fractions from an ethylene–octene copolymer and an ethylene–butene copolymer, respectively, using boiling hexane ( $68.7^\circ\text{C}$ ) as the solvent. EH is an extracted fraction from an ethylene–hexene copolymer using boiling octane ( $125.7^\circ\text{C}$ ) as the solvent. Filtration was performed using  $1.0\text{ }\mu\text{m}$  filters from Millipore. The powder-like material left after filtration was dried overnight in an oven at  $30^\circ\text{C}$  followed by 48 h in a vacuum exicator at  $30^\circ\text{C}$ .

#### 2.5. Blend preparation

Blends with varying ratio of the blend components were made by dissolving both components in boiling xylene under constant stirring for at least 40 min. followed by co-precipitation in an excess amount of cold methanol, a non-solvent. Filtration and drying were thereafter performed as described above. A blend containing  $x\text{ wt}\%$  of LPE(26k) and  $y\text{ wt}\%$  of EB1(7.7) will be denoted  $x/y$  LPE(26k)/EB1(7.7).

#### 2.6. Quenching

Films, approximately  $50\text{ }\mu\text{m}$  in thickness were made in a Graseby Specac IR film press at  $170^\circ\text{C}$  by allowing the material to melt in the press, followed by a pressure sequence of a few seconds. The samples were then taken out from the press and cooled down to room temperature in air. Quenched samples for DSC were obtained by encapsulating one single flat and circular film (being  $50\text{ }\mu\text{m}$  in thickness and weighing 1 mg) in an aluminium DSC sample pan. The sample pan was thereafter wrapped in one thin layer of aluminium foil and immersed into a silicon oil bath at a predetermined temperature. After 30 min the

samples were put as quickly as possible into methanol at its freezing point ( $-98^\circ\text{C}$ ). The sample pans were then cleaned to avoid contamination from the silicon oil. Quenching of samples for DSC was also performed by putting the samples (encapsulated in DSC sample pans) as quickly as possible from the lower hot surface in a Schwabenthan polystat 200T hot press into cold methanol. This was done to detect possible differences between results obtained from the method involving the silicon oil bath and results obtained using the hot surface.

Quenched samples for TEM were obtained by putting a thin flat film between thin glass cover slips. The film was then immersed into the silicon oil bath and thereafter quenched.

Results presented by [14] indicate that the type of phase separation observed is dependent on the storage time in the melt. When the melt is held for times less than 25 min, the separated phases are observed to be smaller and more wide-spread. These small separated domains are observed to ripen with storage time in the melt. A storage time of 30 min was therefore used to ensure that equilibrium conditions were reached in the melt prior to quenching.

The actual cooling rate the samples experience during the quenching is difficult to measure, since the samples are encapsulated in DSC sample pans. A cooling rate higher than  $1000^\circ\text{C}/\text{min}$  has been suggested [20], based on visual observations, in experiments where the DSC pan is flicked from a hot bench into acetone at its freezing point. The real cooling rate is probably lower due to heat of fusion in the sample.

#### 2.7. DSC

Thermal examination of the quenched blends was performed with a Perkin–Elmer DSC-7 flushed with nitrogen and equipped with a water-cooling unit. A small piece of aluminium sheet of mass 1.0 mg was placed in the reference pan. This will eliminate the mass difference between the sample and reference and give rise to a more stable baseline [36]. The samples were heated from 10 to  $150^\circ\text{C}$  at a heating rate of  $10^\circ\text{C}/\text{min}$ . In cases where reorganisation peaks are believed to occur, the cooling and heating rates were varied to verify the nature of these peaks. If the ratio of the two melting peaks is found to be highly dependent on the heating rate applied, reorganisation effects are believed to be responsible for the splitting. No difference among the samples due to thermal lag during the heating scan are believed to occur, since the films used for DSC were thin ( $\approx 50\text{ }\mu\text{m}$ ) and care was taken to ensure that the geometry of each film (circular) was equal [36]. Calibration was regularly checked against the onset melting temperature of a pure Indium sample using the same heating rate as employed in the measurements. The baseline was regularly checked using empty sample pans. DSC melting scans were also performed on films originally meant for TEM, to explore whether the films quenched for TEM (put between

thin glass cover slips) behave different in DSC compared to films quenched for DSC (sealed in DSC sample pans). No such difference was observed.

### 2.8. TEM

The quenched films were cut into rectangular shape, put in glass tubes and chlorsulfonic acid was added. The samples were held in the acid at room temperature for times between 5 and 20 days. The actual time depends on the sample, since the rate of staining of the acid decreases with increasing crystallinity of the sample. Several fixing times were employed on each sample to ensure that no information was lost due to lamellae degradation in the samples [20,37] and to avoid crystal shrinkage [38,39]. The samples were thereafter cleaned and embedded in an epoxy resin. After trimming, the samples were mounted in a Reichert-Jung ultramicrotome operated at room temperature. Thin sections, approximately 70 nm in thickness were allowed to float onto a small water bath glued to a sharp glass knife. The sections were for practical reasons gathered from a cross-section of the samples. Since the surface of the samples experiences the fastest cooling rate, this procedure might be less good. However, the interior of the sections seemed to exhibit a similar morphology as the edges, in accordance to observations by others [5]. The sections were thereafter put on TEM grids and allowed to float in a 1% water solution of uranyl acetate for 2 h to enhance contrast.

Preparation of samples containing small amounts of the linear blend component (less than 40 wt%) was unsuccessful. These samples appeared to be too soft to achieve sections thin enough for TEM by this method. The samples were examined in a Phillips CM30 TEM operated at 300 keV. The thickness of the lamellae was evaluated directly on the negatives, using an ocular and a light table. The thickness of the lamellae was measured at several magnitudes involving a large number of lamellae.

### 2.9. Atomic force microscope

Samples for AFM were quenched in the same way as the samples quenched for TEM. The samples were thereafter etched using the Bristol modification [39] of a sample preparation technique presented by Bassett and Hodge [40,41]. Several etching times were employed on each sample in order to optimise the structure. The samples were thereafter washed according to published procedures [39]. The AFM measurements were performed with a NanoScope IIIa, Multimode™ SPM from Digital instruments. Calibration of the instrument was performed by scanning a calibration grid with precisely known dimensions. All scans were performed in air with commercial Si Nanoprobes™ SPM Tips. Height and phase imaging were performed simultaneously in Tapping mode at the fundamental resonance frequency of the Si cantilever with typical scan rates of 0.5–1.0 line/s using j-type scan heads. The

free oscillating amplitude was 3.0 V, while the setpoint amplitude was chosen for each sample, typically in the range from 2.0 to 2.4 V.

### 2.10. Morphology maps

In order to handle the large amount of experimental data obtained using the method of quenching, so-called morphology maps were constructed [1–22]. Several examples of such constructions will be given later in the text (an example is given in Fig. 5). The morphology map is simply a co-ordinate system, where the  $x$ -axis gives the amount (in wt%) of the linear component in the blend. The  $y$ -axis gives the temperature from which the melt was quenched. A particular blend, quenched from a particular temperature determines a co-ordinate ( $x,y$ ) in the morphology map. The co-ordinate ( $x,y$ ) will be given the letter “M” if the DSC and TEM results indicate that this particular blend is homogeneous in the melt prior to quenching. The letter “S” will be used to indicate that the blend is separated. These constructions represent a very elegant way to handle large amounts of experimental data. A large number of morphology maps have been constructed earlier by others [1–22], based on blends of linear and lightly branched polyethylenes. These morphology maps are found to show characteristic behaviour that will be listed briefly below.

Unless the molecular weight of the linear component in the blend is very low ( $2 \times 10^3$  g/mol [3,4]), the blends show phase separation of a characteristic type. A closed loop of phase separation (with an upper and lower critical temperature) is present for low LPE content. The extent of this phase separation (the compositional range over which this phase separation is observed) is found to depend on several factors. It is found to be reduced if the amount of comonomer in the branched blend component is increased [7,9,11,16] and if the molecular weight of the linear component is reduced (in the range below 50 000 g/mol. Above 50 000 g/mol the extent of phase separation only changes slowly [3,4]). The amount of short chain branches in the branched blend component is found to be the most important factor to the extent of phase separation [7,11,16,17,22]. The type of short chain branches is found to be of only secondary importance. It has furthermore been observed that blends of two near random lightly branched copolymers result in morphology maps similar to blends of an LPE and a random copolymer [9,11,14,16]. Furthermore, single-site materials are found to behave in the same manner as Ziegler–Natta based materials [18,22].

## 3. Results and discussion

As described in the experimental part, the quenched blends are examined in the solid state using DSC and TEM which represent the basis for construction of the morphology maps. The interpretations of the DSC and TEM observations are therefore important to the overall

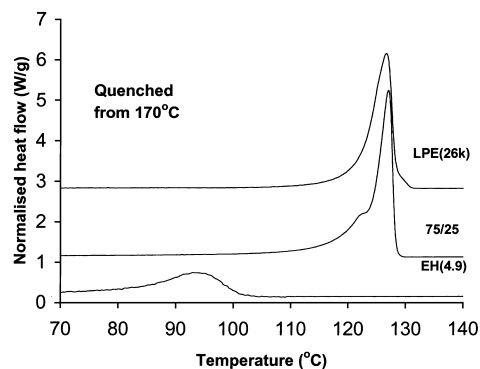


Fig. 1. DSC melting scans of the LPE(26k) blend component, the blend 75/25 LPE(26k)/EH(4.9) and the EH(4.9) blend component, all quenched from 170°C. The heating rate applied was 10°C/min.

appearance of these morphology maps. Two melting peaks in DSC, where the ratio of the peaks is independent of the heating rate applied, are believed to represent melting of two different crystal populations. This observation is believed to indicate that the melt prior to quenching consists of separated domains, where the minority domain mainly contains the LPE component dispersed in a matrix of mainly the branched blend component [1–22]. In the same way, one single well-defined melting peak is believed to represent melting of one crystal population.

The observation of well-separated domains of thicker lamellae in a matrix of thinner lamellae in TEM and/or AFM is believed to indicate the presence of a double

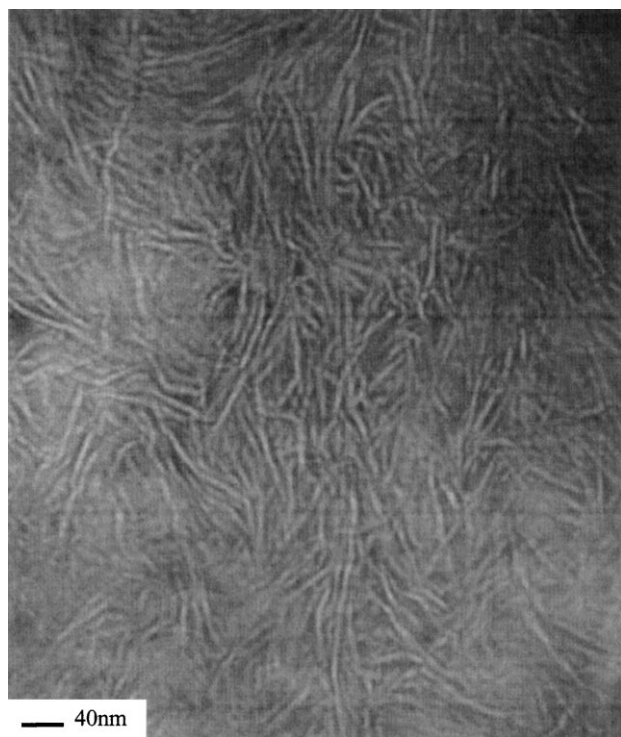


Fig. 2. TEM picture of the blend 75/25 LPE(26k)/EH(4.9) quenched from 170°C.

morphology, due to a separated melt prior to quenching. A single morphology observed in TEM and/or AFM is believed to indicate a homogeneous melt prior to quenching.

### 3.1. DSC and TEM — example of single morphology

Fig. 1 shows a DSC heating scan of the pure LPE(26k) component, the pure EH(4.9) component and the blend 75/25 LPE(26k)/EH(4.9), all quenched from 170°C. The pure LPE(26k) component shows a well-defined single melting peak at 126.6°C. The pure EH(4.9) component shows a rather broad melting peak at 95°C. The 75/25 blend of these two components shows one single well-defined melting peak at 127.3°C. No trace after the EH(4.9) blend component is found. This result indicates that only one crystal population is present in this blend, which is believed to indicate that the melt was homogeneous prior to quenching. A shoulder is, however, visible on the melting peak of the blend. This type of shoulder is observed for almost every blend containing more than 25% (by weight) of the linear blend component. For lower amounts of the linear blend component, a splitting into two melting peaks is observed. However, it turns out that the ratio of the shoulder and the main melting peak, shown in Fig. 1, shows a characteristic dependency on the heating and cooling rates applied. This is especially obvious when the amount of the linear component in the blend is low, i.e. lower than 40% (by weight), where the shoulder is enhanced. This behaviour has been discussed elsewhere [32–34,36,42–44], and is believed to be explained from reorganisation of crystalline material during the melting. The shoulder observed in the blend LPE(26k)/EH(4.9) shown in Fig. 1, and similar splitting of melting peaks found in other blends are therefore not considered as being linked to the melt prior to quenching, but rather to effects that occur during the melting.

Fig. 2 shows a TEM-picture of the blend 75/25 LPE(26k)/EH(4.9), quenched from 170°C, the same blend that was shown in Fig. 1. Lamellae of uniform appearance and thickness distribution are found which indicate a single morphology, in accordance with the DSC results in Fig. 1. Based on these results, it is believed that the blend 75/25 LPE(26k)/EH(4.9) was homogeneous in the melt prior to quenching.

### 3.2. DSC and TEM — indications of double morphology

Fig. 3 shows DSC melting peaks of the pure EH(3.9) component and the blend 40/60 LPE(26k)/EH(3.9), quenched from 140°C. The EH(3.9) blend component shows a rather broad melting peak at 98°C, while the blend 40/60 LPE(26k)/EH(3.9) shows two separate melting peaks, a small peak at 96°C, and a much more prominent peak at 123.5°C (cut in this figure). The position and appearance of the small melting peak in the blend 40/60 LPE(26k)/EH(3.9) indicate that this peak represents melting of mainly the EH(3.9) component. The small melting peak occurs, however, at slightly lower temperatures than observed for the pure EH(3.9) blend component. This has been observed

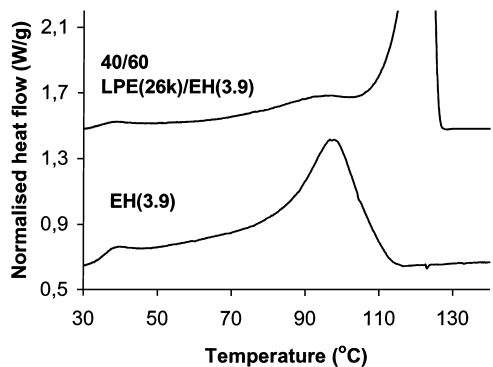


Fig. 3. DSC melting scans of the pure EH(3.9) blend component and the blend 40/60 LPE(26k)/EH(3.9), quenched from 140°C. The heating rate applied was 10°C/min.

in similar blends and discussed elsewhere [34]. The position and appearance of the major melting peak in the blend 40/60 LPE(26k)/EH(3.9) indicate that this peak represent melting of an LPE(26k)-rich component. The position of this peak occurs at a lower temperature than the pure LPE1(26k) blend component, an observation that most probably has a complex explanation and is discussed elsewhere [34,45]. The ratio of the two melting peaks in the blend 40/60 LPE(26k)/EH(3.9) is found to be stable when the heating and cooling rates are varied in a systematic way, an observation that most probably exclude reorganisation during heating as an explanation. It is therefore believed that the blend 40/60 LPE(26k)/EH(3.9) consists of two separate

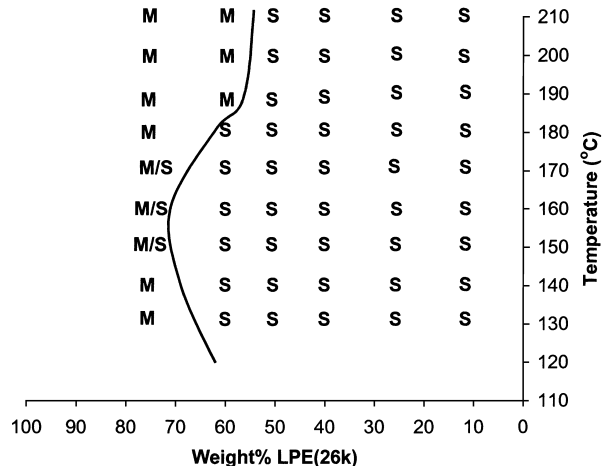


Fig. 5. Morphology map of the blend system LPE(26k)/EO(4.8).

crystal populations, a result that indicate a separated melt prior to quenching.

Fig. 4 shows an AFM picture of the blend 40/60 LPE(26k)/EH(3.9) quenched from 140°C. Two different morphologies are found in this picture. Less developed banded-spherulites with lamellae radiating out from the centre are found in a matrix of thinner lamellae. A part of such a spherulite is shown in the upper left corner in Fig. 4. The banded spherulites are observed to be a few microns in diameter and are separated on a similar scale. The two horizontal stripes without contrast in the figure are artefacts

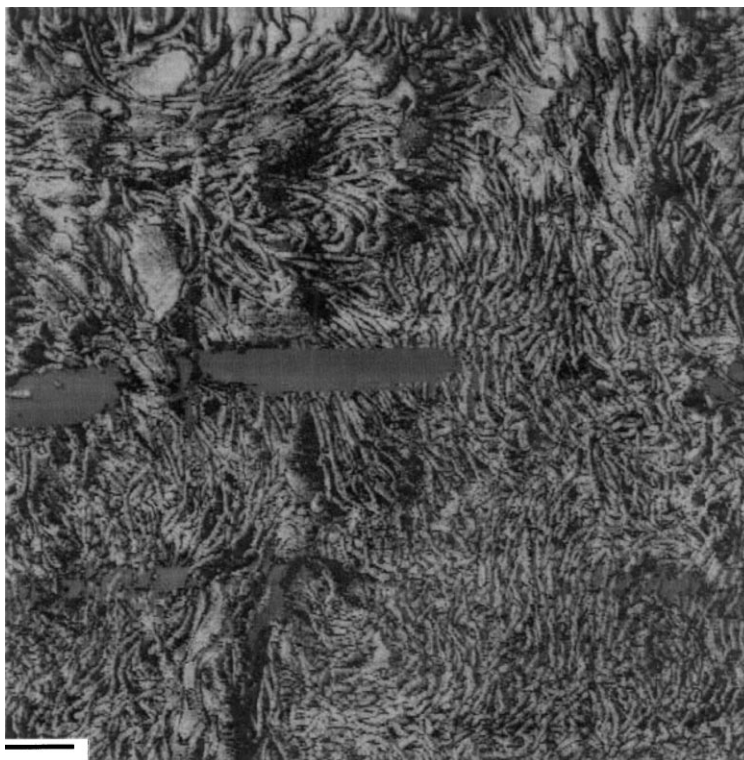


Fig. 4. AFM phase contrast picture of the blend 40/60 LPE(26k)/EH(3.9), quenched from 140°C. The scale bar shown in the picture is 0.5 μm.

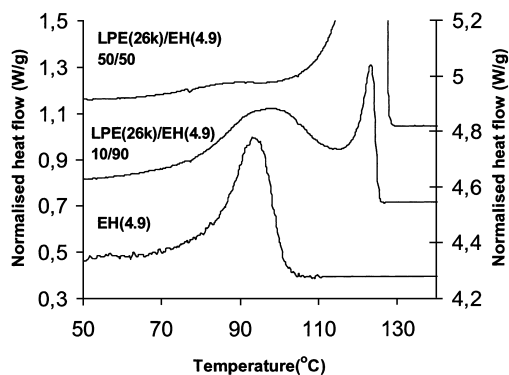


Fig. 6. DSC heating scans of the pure EH(4.9) blend component, the blend 10/90 LPE(26k)/EH(4.9) and the blend 50/50 LPE(26k)/EH(4.9), all quenched from 200°C. The heating rate applied was 10°C/min. The blend 50/50 LPE(26k)/EH(4.9) uses the right vertical axis, while the other DSC endotherms use the left vertical axis.

most probably due to materials adhered to the tip for a short period or drift in the drive amplitude during examination. The morphology shown in Fig. 4 is in agreement to the DSC results in Fig. 3, and is believed to indicate that the melt prior to quenching was separated.

### 3.3. Morphology maps

Based on results similar to the blend systems presented above, morphology maps are constructed as described in the experimental part in this text. A complete morphology map for the blend system LPE(26k)/EO(4.8) is shown in Fig. 5. As the diagram indicates, there seems to be a wide region of phase separation in the melt in this blend system. The region of phase separation is wide in both composition and temperature. A homogeneous melt is only found when the

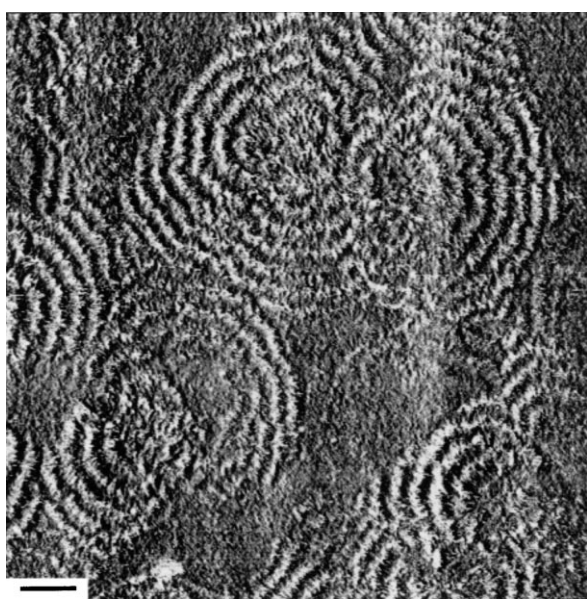


Fig. 7. AFM phase contrast picture of the blend LPE(26k)/EH. The scale bar shown in the picture is 3.0 μm.

amount of the linear component in the blend is high. The region of phase separation has not the shape of a closed loop, which others have found to be a characteristic feature of resembling blend systems [1–22]. The homogeneous region seems, however, to increase as the temperature (from which the melt was quenched) increases, indicating a closed loop for much higher temperatures. No attempts were, however, made to increase the temperature any further, due to the possibility of degradation at such high temperatures. Early results suggested that the linear blend components were able to crystallise isothermally at temperatures below 130°C. Quenching from temperatures below 130°C was therefore not performed. The region of phase separation is found to be significantly wider in both temperature and composition compared to results presented earlier by others [1–22].

The morphology map presented in Fig. 5 is therefore quite different from the morphology maps presented earlier, i.e. no closed loop of phase separation is present and the phase separation is much wider in both composition and temperature. As will become clear later in the text, most of the morphology maps constructed in this work show the same principal behaviour as the morphology map presented in Fig. 5. The explanation of the obvious difference in the overall appearance of the morphology maps presented here compared to morphology maps presented earlier by others is not clear. Different possible explanations will be suggested below. The first explanation governs the interpretation of the DSC and morphology data.

DSC results obtained for the blends 10/90 LPE(26k)/EH(4.9) and 50/50 LPE(26k)/EH(4.9), quenched from 200°C are presented in Fig. 6. These results are believed to be a rather clear indication of two-component structures in these blends. The position of these blends in the morphology map is far outside the region of closed loop of phase separation found by others [1–22]. The occurrence of two separate melting peaks is particularly clear in the blend 10/90 LPE(26k)/EH(4.8) while the smallest melting peak in the blend 50/50 LPE(26k)/EH(4.9) is almost invisible unless the y-axis is expanded.

Furthermore, differences might occur due to the sample preparation and interpretation of the TEM results. Results published by others [1–22] are based on a modified version [39] of a sample preparation technique presented by Bassett and Hodge [40,41] (a procedure used for preparation of samples for AFM in this work). Surface replicas are obtained from samples etched in permanganic acid. As described in the experimental part of this text, stained sections for TEM were obtained in this work using chlor-sulfonic acid following the method of Kanig [46,47]. Crucial information about the sample morphology might be lost in both sample preparation techniques, especially the thinner lamellae. These are more susceptible to degradation when chlor-sulfonic acid is employed, while the problem with detached material could obscure the interpretation of the surface replicas.

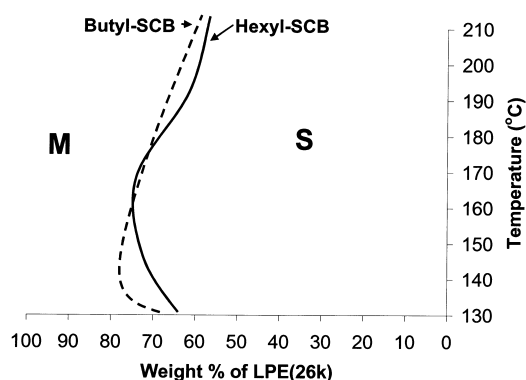


Fig. 8. Morphology maps of the blend systems LPE(26k)/EH(4.9) and LPE(26k)/EO(4.8).

Furthermore, the observation of separate domains of banded and unbanded domains in TEM should not alone be taken as an argument in favour of phase separation in the melt. Fig. 7 shows a phase picture of the blend 10/90 LPE(26k)/EH, obtained by AFM. Banded and unbanded domains are found that are separated on a micron scale. However, the lamellae thickness distribution, involving lamellae in both banded and unbanded regions is found to be rather uniform (due to the magnification, the lamellae are hardly visible in Fig. 7). This observation is confirmed from DSC. The DSC melting curve of the blend in Fig. 7 shows one relatively sharp, single melting peak, indicating the presence of only one crystal population. The blend in Fig. 7 clearly demonstrates that the presence of banded and unbanded regions should not be directly linked to the presence of two crystal populations.

Another possible source to the observed differences in the morphology maps is the actual cooling rate achieved in the procedure of quenching. As described in the experimental part of this text, the samples for DSC were sealed in DSC sample pans, wrapped in one thin layer of aluminium foil before being immersed into the silicone oil bath and thereafter quenched. This procedure should be compared to the

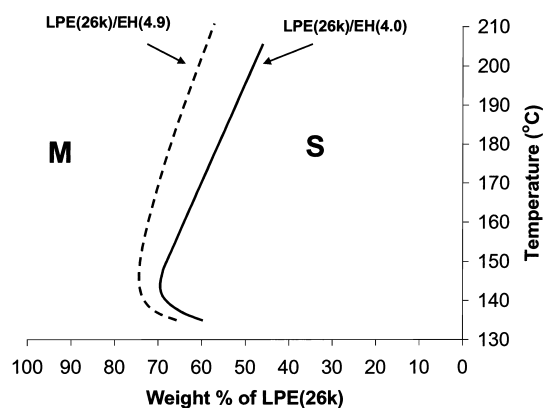


Fig. 9. Morphology maps of the blend systems LPE(26k)/EH(4.9) and LPE(26k)/EH(4.0).

procedure described by others. Morgan et al. [20] use DSC sample pans held on a Kofler hot bench before quenching. This procedure will probably give a faster cooling rate compared to the cooling rate obtained using oil bath, which was done in this study. However, since the blend components are found to separate on a micron scale in the melt prior to quenching, a small difference in the cooling rate should not influence the results significantly. As an alternative to the method involving the silicone oil bath, the samples, encapsulated in DSC pans, were held on the hot surface of a Schwabentan Polystat press before quenched in methanol. This procedure should give cooling rates comparable to the cooling rates obtained using a Kofler hot bench. No difference in DSC melting curves were, however, detected between samples held in the press and samples held in the oil bath. The oil bath was preferred because the temperature control of the press was not considered as good enough.

The third suggestion governs the temperatures from which the melt is quenched. In this work care is taken to ensure that the melt is quenched from temperatures where both blend components are completely melted. Blends made from these components are then kept in the melt at temperatures sufficiently higher than the melting point of the blend components. This will ensure that no crystallites are left that will anneal during storage in the melt and subsequently self-seed the samples during the rapid cooling. The experience gained from this work is that an incomplete melting of one of the blend components (while the other is completely melted) will result in a separated melt, as judged from DSC and TEM/AFM.

The final suggestion which perhaps is the most important factor to explain the wide regions of phase separation observed in the blends used in this work, is the fact that single-site materials are used as blend components. The more even distribution of short chain branches along the polymer chains (and less variations among different chains) and narrow molecular weight distribution compared to ordinary Ziegler–Natta based materials, will most probably influence the phase behaviour in the melt. In Ziegler–Natta based materials, there exist linear chain segments in the branched blend components, even for relatively high amount of comonomer incorporation. This will probably make the Ziegler–Natta based blend components more compatible in the melt as compared to single-site based blend component. It is therefore expected that single-site materials will lead to phase separation in the melt that is wider at least in composition of the blends.

#### 3.4. The effect of type of short chain branches in the copolymer

In Fig. 8, morphology maps obtained from two different blend systems are compared. The thick line indicates the area of phase separation observed in the LPE(26k)/EO(4.8) blend system, while the dotted lines indicate the



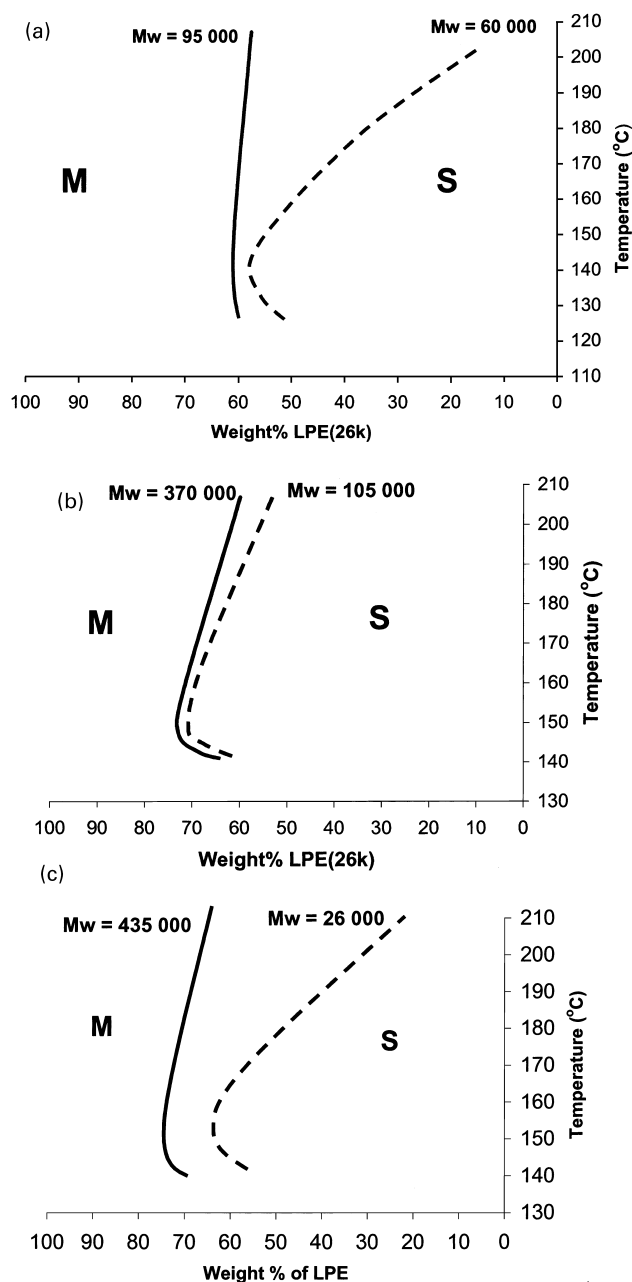


Fig. 10. Morphology maps of the blend systems: (a) LPE(26k)/EB1(7.7) and LPE(26k)/EB2(7.7); (b) LPE(26k)/EH(3.9) and LPE(26k)/EH(4.0); and (c) LPE(26k)/EB1(7.7) and LPE(435k)/EB1(7.7).

area of phase separation observed in the LPE(26k)/EH(4.9) blend system. The only main difference between these blend systems is the type of short chain branches in the branched blend components (see Table 1 for details). The extent of phase separations is found to be almost equal in these blend systems, i.e. the type of short chain branches seems to be of less importance to the extent of phase separation. This result has also been indicated by others [7,11,16,17]. It is furthermore observed that the region of phase separation in both blend systems is significantly wider than earlier reported in resembling blend systems.

### 3.5. The effect of varying the comonomer content of the copolymer

Fig. 9 compares the morphology maps obtained from the blend systems LPE(26k)/EH(4.0) and LPE(26k)/EH(4.9). The main difference among these blend systems is the amount of comonomer in the branched blend component, see Table 1 for details. The result in Fig. 9 indicates that the extent of phase separation is reduced when the amount of comonomer in the branched blend component is reduced. In addition to the results presented in Fig. 9, results from preliminarily DSC experiments in blends of LPE(26k) and an ethylene–hexene copolymer containing 1.8 mol% comonomer indicated a very limited (if any) region of phase separation, an observation in accordance with the observations in Fig. 9. The amount of comonomer in this sample is, however, probably too low to enable the observation of two separate melting peaks in DSC [34]. By further decreasing the amount of comonomer, the extreme limit is reached as the amount of comonomer is reduced to zero. This represents a blend of two linear polymers. The LPE(26k)/LPE(435k) blend system was examined and found to be completely homogeneous in the melt, even though the difference in molecular weight among the blend component is considerable. This is in agreement to results presented by others [13]. These results indicate that the extent of phase separation is invariably reduced from a highly separated melt to a completely homogeneous melt as the amount of comonomer in the branched blend component is reduced. Others have observed that the extent of phase separation in the blend is reduced if the amount of comonomer in the branched blend component is increased, in blend systems containing ethylene–octene copolymers [7] and in blends containing ethylene–butene copolymers [16]. It is claimed that this behaviour can be understood if an extra free energy term is added to the usual Flory–Huggins model [8]. These observations are not in accordance with the observation made in the ethylene–hexene blend system reported here.

### 3.6. The effect of varying the molecular weight of the blend components

In Fig. 10a, morphology maps obtained from the blend systems LPE(26k)/EB1(7.7) and LPE(26k)/EB2(7.7) are compared. The only main difference between the blends is the molecular weight of the branched blend component, see Table 1. The results in Fig. 10a suggest that the extent of phase separation is significantly wider in the LPE(26k)/EB2(7.7) blend system compared to the LPE(26k)/EB1(7.7) blend system. This result indicates that the molecular weight of the branched blend component is important to the extent of phase separation, i.e. the extent of phase separation is increased when the molecular weight of the branched blend component is increased.

When the molecular weight of the branched blend component is increased beyond 100 000 g/mol, the extent

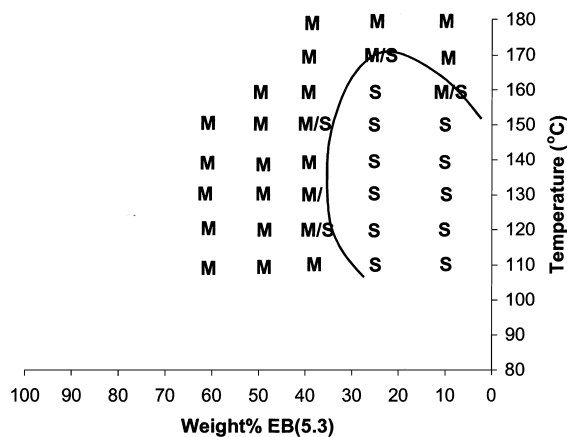


Fig. 11. Morphology map of the blend system EB(5.3)/EB2(7.7).

of phase separation is observed to be approximately fixed. This is illustrated in Fig. 10b, where the LPE(26k)/EH(3.9) and LPE(26k)/EH(4.0) blend systems are compared. The extent of phase separation is found to be only slightly increased in LPE(26k)/EH(3.9), where the molecular weight of the branched blend component is 370 000 g/mol compared to LPE(26k)/EH(4.0), where the molecular weight is 105 000 g/mol. In Fig. 10c, morphology maps obtained from the blend systems LPE(26k)/EB1(7.7) and LPE(435k)/EB1(7.7) are compared. The only main difference between the blends is the molecular weight of the linear blend component, see Table 1. The results in Fig. 10c suggest that the extent of phase separation is significantly wider in the LPE(435k)/EB1(7.7) blend system compared to the LPE(26k)/EB1(7.7) blend system. This result indicates that the molecular weight of the linear blend component is important to the extent of phase separation, i.e. the extent of phase separation is increased when the molecular weight of the linear blend component is increased.

As discussed in the previous section, a blend of two linear components results in a homogeneous blend, even though the difference in molecular weight is significant. This result strongly suggests that a difference in molecular weight among the blend components is not alone enough to cause phase separation in the melt. A similar result is obtained when two copolymers with different molecular weight (having similar type and amount of branches) are blended. The EH(3.9)/EH(4.0) blend system was investigated and found to be homogeneous in the melt for all temperatures and blend compositions.

### 3.7. The effect of blending different copolymers

In Fig. 11, a morphology map of the EB(5.3)/EB2(7.7) blend system is shown. The only difference between the blend components is the amount of comonomer, see Table 1. The morphology map in Fig. 11 does not resemble any of the other morphology maps constructed in this work, i.e. the

region of phase separation is significantly reduced (in both composition and temperature) compared to the other blend systems presented here. In fact, the morphology map in Fig. 11 resembles morphology maps presented by others [1–22], constructed from blends of linear and branched polyethylene. Others have found that blends of two lightly branched near randomly copolymers behave like a blend of a linear and lightly branched polyethylene [9,11,14,16], which is not in accordance to the results presented here. Furthermore, the extent of phase separation in the blend shown in Fig. 11 is wider in temperature than results presented by others on similar blend systems [22].

## 4. Conclusions

In this work, quenched blends of different single-site based LPEs with several single-site ethylene–1-alkene copolymers are studied by DSC, TEM and AFM. The aim of this work has been to explore how the molecular weight of the blend components and the type and amount of comonomer in the branched blend components affect the extent of phase separation in the melt in these blends. Based on the materials employed and the experimental procedures that are followed, the following conclusions are reached:

- The extent of phase separation is found to be wider (both in temperature and composition) than observed earlier. Furthermore, no clear indications of the existence of a closed loop of phase separation are observed in the blend systems. However, the phase separation is found to be limited in composition and partly by temperature. This difference might be partly explained from the more narrow distribution of comonomer and molecular weights that is present in single-site materials compared to materials made from ordinary Ziegler–Natta based processes.
- The type of short chain branches (for fixed  $M_w$  and amount of comonomer) is found to be of little (if any) importance. This is in accordance with previously published results.
- The extent of phase separation is found to be reduced if the amount of comonomer in the branched blend component is reduced (for fixed  $M_w$  and type of comonomer), in blends containing ethylene–hexene copolymers. Others have reached the opposite conclusion in blend containing ethylene–octene copolymers and ethylene–butene copolymers.
- If the difference in  $M_w$  between the blend samples is increased, the extent of phase separation is found to increase (for fixed type and amounts of comonomer). This conclusion is independent of the blend component that increases (compared to the other blend component).
- In blends of two LPE with a considerable difference in  $M_w$ , no phase separation is observed. A homogeneous

melt is also found in a blend of two copolymers with equal amounts of comonomer (for fixed type and amount of comonomer). These results indicate that a difference in  $M_w$  among the blend components is not enough by itself to initiate phase separation in the melt.

- In a blend of two ethylene–butene copolymers with different amounts of comonomer (for fixed  $M_w$ ), the extent of phase separation is significantly reduced in both temperature and composition compared to blends of an LPE and similar copolymers investigated in this work.

## Acknowledgements

Financial support from the Norwegian Research Council (NFR) under the Polymer Science Program is gratefully Acknowledged. The authors also want to thank Heidi Normes Bryntesen at Borealis for GPC measurements, Arja Lehtinen at Borealis for FTIR measurements, Per Eugene Kristiansen for NMR measurements and Irene Helland at Borealis for help with characterisation and generation of materials.

## References

- [1] Barham PJ, Hill MJ, Kelley A, Rosney CCA. *J Mater Sci Lett* 1988;1271.
- [2] Hill MJ, Barham PJ, Kelley A, Rosney CCA. *Polymer* 1991;32:1384.
- [3] Hill MJ, Barham PJ, Kelley A. *Polymer* 1992;33:2530.
- [4] Hill MJ. *Polymer* 1991;35:1994.
- [5] Hill MJ, Barham PJ. *Polymer* 1992;33:4099.
- [6] Hill MJ, Barham PJ. *Polymer* 1992;33:4891.
- [7] Hill MJ, Barham PJ, van Ruiten J. *Polymer* 1993;34:2975.
- [8] Barham PJ, Hill MJ, Goldbeck Wood EG, van Ruiten J. *Polymer* 1993;34:2981.
- [9] Thomas D, Williamson J, Hill MJ, Barham PJ. *Polymer* 1993;34:4919.
- [10] Hill MJ, Organ SJ, Barham PJ. *Thermochim Acta* 1994;17:238.
- [11] Hill MJ, Barham PJ. *Polymer* 1994;35:1802.
- [12] Puig CC, Odell JA, Hill MJ, Barham PJ, Folkes MJ. *Polymer* 1994;35:2452.
- [13] Hill MJ, Barham PJ. *Polymer* 1995;36:1523.
- [14] Hill MJ, Barham PJ. *Polymer* 1995;36:3369.
- [15] Schipp C, Hill MJ, Barham PJ, Cloke V, Higgins JS, Oiarabal L. *Polymer* 1996;37:2291.
- [16] Morgan R, Hill MJ, Barham PJ, Frye C. *Polymer* 1997;38:1903.
- [17] Hill MJ, Morgan R, Barham PJ. *Polymer* 1997;38:3003.
- [18] Hill MJ, Barham PJ. *Polymer* 1997;38:5595.
- [19] Hill MJ, Morgan RL, Barham PJ. *J Macromol Sci, Phys* 1999;B38:37.
- [20] Morgan R, Hill MJ, Barham PJ. *Polymer* 1999;40:337.
- [21] Morgan RL, Hill MJ, Barham PJ, van der Pol A, Kip B, van Ruiten J, Markwort L. *J Macromol Sci, Phys* 1999;38(4):419.
- [22] Hill MJ, Barham PJ. *Polymer* 2000;41:1621.
- [23] Schipp C, Hill MJ, Barham PJ, Cloke VM, Higgins JS. *Polymer* 1996;37:2292.
- [24] Alamo RG, Londono JD, Mandelkern L, Stehling FC, Wignall GD. *Macromolecules* 1994;27:411.
- [25] Bates FS, Wignall GD, Koehler WC. *Phys Rev Lett* 1985;55:2425.
- [26] Krishnamoorti R, Graessley WW, Balsara NP, Lohse DJ, Butera RJ, Fetters LJ, Schulz DN, Sissano JA. *Macromolecules* 1994;27:2574.
- [27] Londono JD, Narsten AH, Honnell KG, Hsieh ET, Johnson TW, Bates FS. *Macromolecules* 1994;27:2864.
- [28] Nicholson JC, Finerman TM, Christ B. *Polymer* 1990;31:2287.
- [29] Tashiro K, Imanishi K, Izuchi M, Kobayashi M, Itoh Y, Ima M, Yamaguchi Y, Ohashi M, Stein RS. *Macromolecules* 1995;28:8484.
- [30] Wignall D, Alamo RG, Londono JD, Mandelkern L, Stehling FC. *Macromolecules* 1996;29:5332.
- [31] Lee SY, Jho JY, Huh W. *J Ind Engng Chem* 1998;4(3):258.
- [32] Zhao Y, Liu S, Yang D. *Macromol Chem Phys* 1997;198:1427.
- [33] Tanem BS, Stori AA. *Thermochim Acta* 2000;345:73.
- [34] Tanem BS, Stori AA. Submitted for publication.
- [35] Hansen EW, Blom R, Bade OM. *Polymer* 1997;38:4295.
- [36] Behrstein VA, Egorov VM. In: Kemp TJ, Kennedy JF, editors. *Differential scanning calorimetry of polymers*, Prentice Hall Series in Polymer Science and Technology. Chichester, UK: Ellis Horwood, 2001 (Sections 1 and 5).
- [37] Martinez-Salazar J, López Cabarcos E, Rueda DR, Cagiao ME, Baltá Calleja FJ. *Polym Bull* 1984;12:269.
- [38] Hill MJ, Bradshaw DC, Chevili R. *Polym Commun* 1992;33:844.
- [39] Patrick M, Bennett V, Hill MJ. *Polymer* 1996;37(24):5335.
- [40] Olley R, Hodge AM, Bassett DC. *J Polym Sci, Polym Phys* 1979;17:627.
- [41] Bassett DC, Hodge AM. *Proc R Soc A* 1978;359:121.
- [42] Paukkeri R, Lehtinen A. *Polymer* 1993;34(19):4075.
- [43] Paukkeri R, Lehtinen A. *Polymer* 1993;34(19):4083.
- [44] Fonesca CA, Harrison IR. *Thermochim Acta* 1997;313:37.
- [45] Puig CC, Hill MJ, Odell JA. *Polymer* 1993;34:3402.
- [46] Kanig G, Kolloid ZZ. *Polymer* 1973;251:782.
- [47] Kanig G. *Prog Colloid Polym Sci* 1975;57:176.